

Synthesis and Characterizations of Zinc Oxide Nanoparticles Using Various Precursors

¹Sridevi K P, ²Sivakumar S, ³Saravanan K

¹Department of Physics, Sri Kailash Women's College, Thalaivasal, Salem, Tamil Nadu, INDIA

²Department of Physics, Government Arts College (Autonomous), Salem, Tamilnadu, INDIA

³Department of Physics, AVS Engineering College, Salem, Tamilnadu, INDIA

Abstract

Zinc oxide nanoparticles were synthesized by sol-gel method using zinc chloride / zinc acetate dihydrate / zinc nitrate hexahydrate and Sodium Hydroxide as precursors. The XRD patterns ZnO nanoparticles reveal the formation of well-crystalline single phase materials and all ZnO nanoparticles possess hexagonal structure. The lattice parameters were calculated from 2 θ values in the X-ray diffraction patterns by using Fullprof program computer programming. From the results, the unit cell parameters (\AA), unit cell volume (\AA^3) and density (g/cm^3) of ZnO were found to be almost same for various precursor used for synthesis. This confirms, the lattice parameters of the oxides do not depend on the precursor composition. The synthesized ZnO nanoparticles have been characterized by X-ray diffraction (XRD), UV-Visible spectroscopy, VSM studies.

Introduction

Ultrafine semiconductors particles are of great scientific interest as they are effectively a bridge between bulk materials and atomic or molecular structures. They possess special properties such as a large surface to volume ratio, increased activity, special electronic properties and unexpected optical properties as they are small enough to confine their electrons and produce quantum effects. During the past decade a considerable effort has been spent in the preparation and investigation of the family of II-VI nanoscale semiconductors due to their fundamental electronic and optical properties. Among all the II-VI compounds, ZnO is attracting tremendous attention due to its interesting properties like wide direct band gap of 3.3eV at room temperature and high exciton bonding energy of 60meV [1-8]. Nano zinc oxide has a wide range of applications in various fields due to its unique and superior physical and chemical properties compared with bulk ZnO. The large specific surface area, high pore volume, low toxicity, nanostructured properties and low cost of nano ZnO [9] make it a promising candidate particularly in catalysts [10], chemical absorbents, as polymer additives, antiwear additives for oil lubricants and advanced ceramics. Zinc oxide nanoparticles have optical, electrical and

photochemical activity, it can be used as photocatalysts, solar energy conversion cells, Ultra Violet (UV) detectors and UV emitting devices, chemical sensors sensitive to chemicals such as alcohol and benzene, and gas sensing materials for many gases such as ammonia, hydrogen and ozone[14][15]. In this work, zinc oxide nanoparticles were synthesized by sol-gel method using zinc chloride, zinc acetate dihydrate, zinc nitrate hexahydrate as precursors[16][17][18]. The synthesized ZnO nanoparticles have been characterized by X-ray diffraction (XRD), UV-Visible spectroscopy, VSM studies. Using the Fullprof program X-ray diffraction of ZnO nanoparticles was analyzed. A good agreement between experimental and simulated patterns was obtained.

Experimental Details

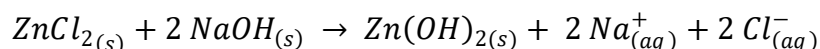
Materials and Methods

The chemicals such as zinc chloride, zinc acetate dihydrate, zinc nitrate hexahydrate, sodium hydroxide, methanol were purchased from Merck and all the chemicals were used as such without any further purification.

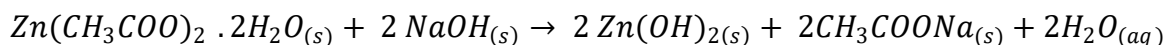
Reaction mechanism



(or)



(or)



and

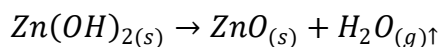


Table 1. Amount of precursor materials (dissolved in 100 ml of water each) used for the preparation of ZnO nanoparticles

Molar concentration	Precursor materials for ZnO	Weight (g)
1	ZnCl ₂	13.67
1	Zn(CH ₃ COO) ₂ · 2H ₂ O	21.95
1	Zn(NO ₃) ₂ · 6H ₂ O	29.74
2	NaOH	8.0

The aqueous solutions of zinc chloride / zinc acetate dihydrate / zinc nitrate hexahydrate [as basic materials] and sodium hydroxide [as precipitator material] were prepared at 1M and dissolved in 100 ml of water each (Table 1). The prepared zinc salt solution was added drop wise into the sodium hydroxide alkaline solution. The above two solutions were mixed perfectly by a magnetic stirring apparatus at room temperature for 2 hours. The dripping of the aqueous alkaline NaOH solution in zinc chloride / zinc acetate dihydrate / zinc nitrate hexahydrate solution results in immediate precipitation of ZnO, and the color changes from transparent to white. Throughout the experiment, the pH was maintained as $\text{pH} > 9$ by the addition of alkali. The solution obtained after complete addition of NaOH was allowed to be under constant stirring for 2 hrs and later sealed and kept overnight. After the whole process zinc hydroxide with some unknown impurities assumed settled at the bottom and the excess mother liquor obtained on top was removed. The remaining solution was centrifuged for 5 mins and the precipitate obtained was washed five times with deionized water and methanol to remove the by products which were bound with the zinc hydroxide and then dried in air atmosphere at about 200°C . After drying $\text{Zn}(\text{OH})_2$ is completely converted into phase pure ZnO material.

Characterization method

The structure of the prepared ZnO nanoparticles was investigated from the X-ray diffraction patterns obtained using a Riagu Mini Flexell Desktop Diffractometer (using $\text{CuK}\alpha$ radiation at a wavelength of 1.5406 \AA). Optical properties were studied using UV-VIS spectrophotometer (JASCO -V-670) in the wavelength range of 300 - 1000 nm. The magnetic properties of the doped thin films were studied using Lake Shore 7404 vibrating sample magnetometer instrument.

Structural analysis

The XRD patterns of the ZnO nanoparticles are shown in Figure 1. The XRD patterns of ZnO nanoparticles reveal the formation of well-crystalline single phase materials. No extra peaks corresponding to any other secondary phases are observed. The obtained XRD patterns of the ZnO were compared with the standard data for ZnO (JCPDS card No. 80-0075). The lattice parameters were calculated from 2θ values in the X-ray diffraction patterns by using Fullprof program computer programming. The results are tabulated in Table 2. From the results, the unit cell parameters (\AA), unit cell volume (\AA^3) and density (g/cm^3) of ZnO were found to be almost same for various precursors used for synthesis. This confirms, the lattice parameters of the oxides do not depend on the precursor composition. Therefore, it is interesting to trace the effect of the precursor composition on the morphology of the ZnO samples and their optical and magnetic properties. XRD data obtained on ZnO using Precursor ZnCl_2 / $\text{Zn}(\text{CH}_3\text{COO})_2 \cdot 2\text{H}_2\text{O}$ / $\text{Zn}(\text{NO}_3)_2 \cdot 6\text{H}_2\text{O}$ are given in Table 3. From the XRD data, it is observed that all ZnO nanoparticles possess hexagonal structure and their corresponding crystallographic data are found to be in line with JCPDS card No. 80-0075. From observed peaks the corresponding planes were indexed in Figure 1 and listed in Table 3.

Table 2 Crystallographic parameters obtained from Fullprof program

Sample	Precursor	Crystal structure	Unit cell parameters (Å)		Unit cell volume (Å ³)	Density (g/cm ³)
			a	c		
ZnO	ZnCl ₂	Hexagonal	3.2504	5.2041	47.6161	5.676
ZnO	Zn(CH ₃ COO) ₂	Hexagonal	3.2499	5.2036	47.5980	5.678
ZnO	Zn(NO ₃) ₂	Hexagonal	3.2536	5.2095	47.7589	5.659

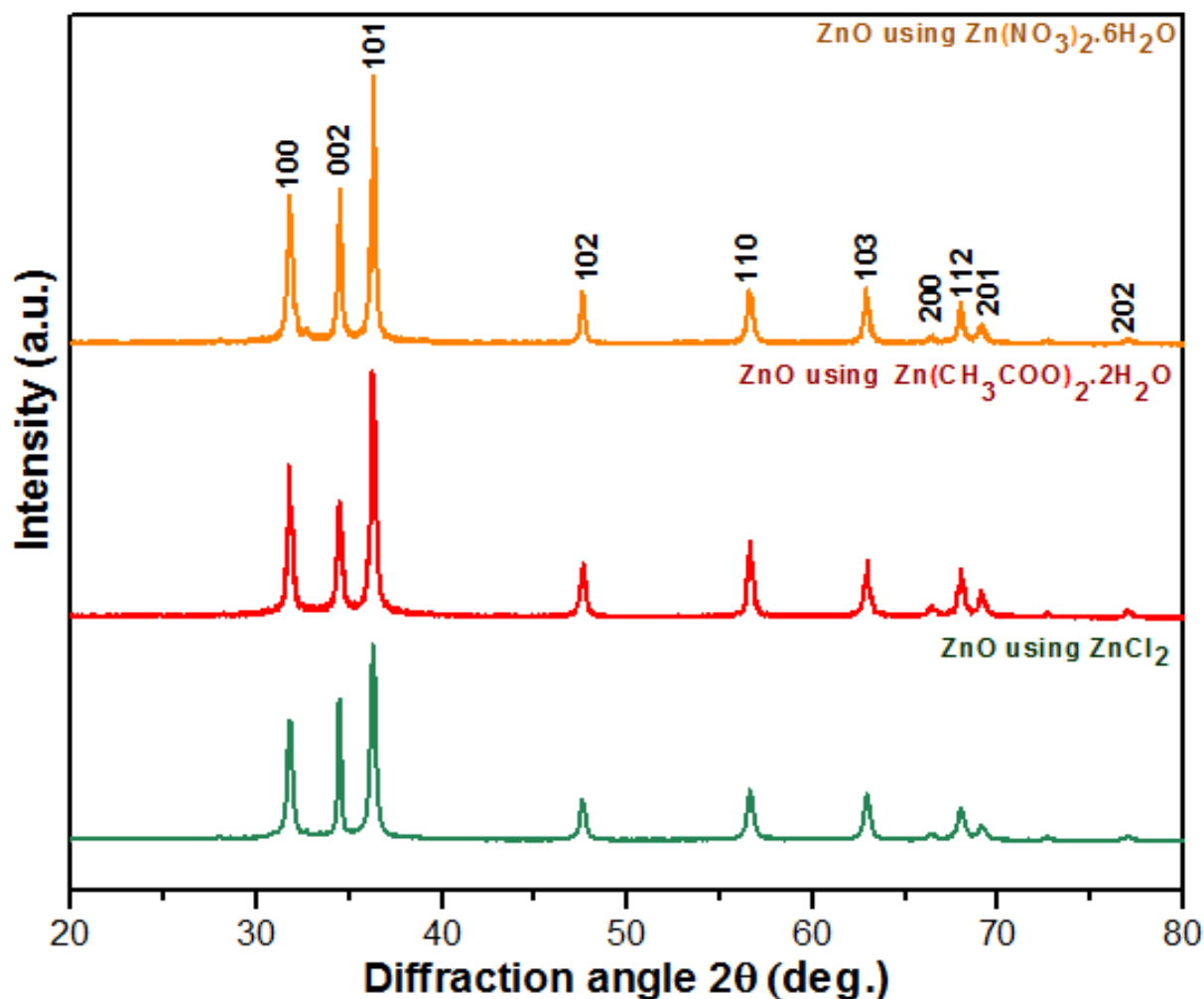


Figure 1 The XRD patterns of the ZnO nanoparticles prepared by using ZnCl₂ / Zn(CH₃COO)₂ · 2H₂O / Zn(NO₃)₂ · 6H₂O

Table 3 XRD data obtained on ZnO using precursor ZnCl_2 / $\text{Zn}(\text{CH}_3\text{COO})_2 \cdot 2\text{H}_2\text{O}$ / $\text{Zn}(\text{NO}_3)_2 \cdot 6\text{H}_2\text{O}$

Standard XRD for ZnO (JCPDS card No. 80-0075)		Observed XRD data for ZnO using Precursor ZnCl_2		Observed XRD data for ZnO using Precursor $\text{Zn}(\text{CH}_3\text{COO})_2 \cdot 2\text{H}_2\text{O}$		Observed XRD data for ZnO using Precursor $\text{Zn}(\text{NO}_3)_2 \cdot 6\text{H}_2\text{O}$	
hkl	d value (Å)	d value (Å)	2 θ value (deg)	d value (Å)	2 θ value (deg)	d value (Å)	2 θ value (deg)
100	2.8179	2.8171	31.76	2.8137	31.80	2.8133	31.81
002	2.6049	2.6040	34.44	2.5992	34.41	2.6008	34.49
101	2.4786	2.4778	36.26	2.4742	36.31	2.4754	36.29
102	1.9128	1.9121	47.56	1.9087	47.65	1.9115	47.57
110	1.6269	1.6264	56.59	1.6271	56.56	1.6281	56.52
103	1.4784	1.4779	62.89	1.4760	62.97	1.4783	62.87
200	1.4089	1.4085	66.37	1.4067	66.47	1.4072	66.44
112	1.3799	1.3796	67.95	1.3778	68.05	1.3791	67.98
201	1.3601	1.3598	69.08	1.3588	69.13	1.3595	69.09
004	1.3024	1.3021	72.61	1.3023	72.59	1.3026	72.57
202	1.2393	1.2383	77.01	1.2378	77.04	1.2380	77.03

Table 4 Structural parameters of ZnO

ZnO precursor	Planes	Peak position 2 θ (°)	FWHM β (°)	Crystallite Size D (nm)	Dislocation Density (δ) (10^{15} lines / m^2)	Stacking faults probability (Å)	Elastic strains ϵ
ZnCl_2	100	31.76	0.3468	24.89	2.6980	0.0029	0.0053
	002	34.44	0.2312	37.60	1.1826	0.0018	0.0033
	101	36.26	0.2890	30.23	1.8292	0.0022	0.0039
$\text{Zn}(\text{CH}_3\text{COO})_2$	100	31.80	0.3472	24.87	2.7037	0.0029	0.0053
	002	34.41	0.2330	37.31	1.2013	0.0018	0.0033
	101	36.31	0.2875	30.40	1.8097	0.0022	0.0038
$\text{Zn}(\text{NO}_3)_2$	100	31.81	0.3476	24.84	2.7098	0.0029	0.0053
	002	34.49	0.2315	37.56	1.1853	0.0018	0.0033
	101	36.29	0.2878	30.36	1.8137	0.0022	0.0038

Dislocations are the imperfections in a crystal and associate with the mis registry of the lattice in one part of the crystal with respect to another part. Unlike vacancies and interstitial atoms, dislocations are not equilibrium imperfections. In fact, the growth mechanism involving dislocations is a matter of importance. Moreover, the dislocation densities of ZnO nanoparticles are calculated. As the dislocation density increases the material become harder. It is observed that the dislocation density (δ) is indirectly proportional to crystallite size (D). The crystallite size, dislocation density, stacking fault and elastic strains values are presented in Table 4. The dislocation density (δ) has been determined using values of lattice constant, FWHM, θ , and crystallite size. The dislocation density, stacking fault and elastic strains are found to be decreased with increase in crystallite size for ZnO using zinc chloride. Furthermore from the calculations, the dislocation density, stacking faults and elastic strains are found to be decreased with increase in crystallite size for ZnO prepared using other precursors. XRD studies showed that, ZnO nanoparticles prepared with various precursor has good crystalline nature, less dislocation, stacking fault and elastic strains. The small value of dislocation density confirms that the sol-gel method is an effective technique for good quality poly crystalline ZnO nanoparticles.

Optical properties

The optical absorption spectra of all synthesized ZnO samples in the ultraviolet and visible spectral ranges demonstrate a displacement of the absorption band edge into the visible region and its dependence on the precursor. The absorption spectra and transmittance spectra of ZnO nanoparticles are shown Figure 2 and Figure 3. The samples exhibit a sharp falling at the absorption edge which is an indication of a good crystallinity. The absorption spectrum of ZnO nanoparticles depends on several parameters such as, method of fabrication, temperature, size and shape. These methods of fabrication result in ZnO nanoparticles that present exciton peak in the range of 355-360 nanometers.

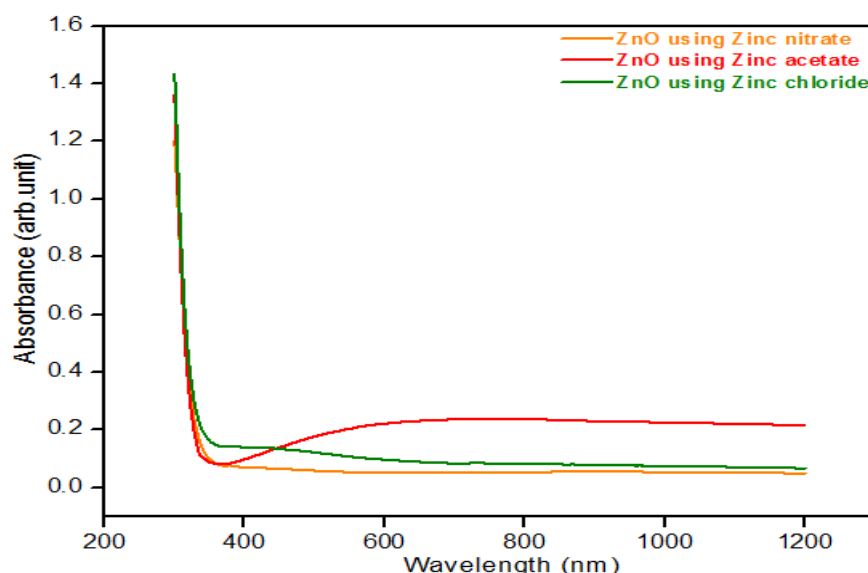


Figure 2 Optical absorbance spectra of ZnO nanoparticles

From the investigations, the absorbance is high in the ultraviolet region and found to be less absorbance above 380 nm in the entire visible region. ZnO produced by zinc chloride has maximum absorbance compared with zinc nitrate and zinc acetate. The transmittance spectrum displayed the excitonic absorption peak at 355-360 nm and have sharp absorption edge which implies the lower particle size of ZnO. The weak and medium absorption area covers almost the whole of the visible field ranging between 600 nm and 800 nm. ZnO produced by zinc nitrate has maximum displacement in transmittance edge of 85% and zinc chloride of 82%. Whereas zinc chloride exhibits the minimal displacement of the transmittance band edge of 60% in visible region.

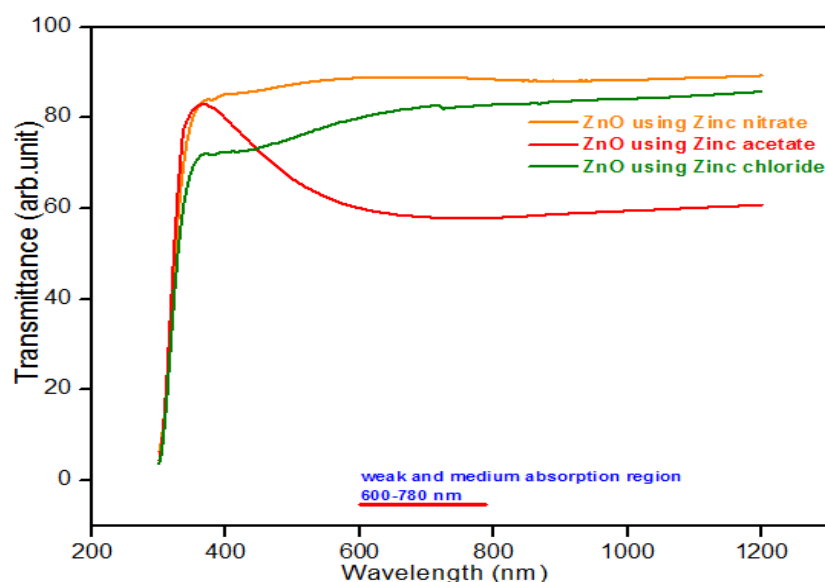


Figure 3 Optical transmittance spectra of ZnO nanoparticles

The band gap values of the sample are determined using the Tauc plot analysis. The optical band gap values have been calculated using the fundamental absorption, which corresponds to electron excitation from the valence band to the conduction band. The relation between absorption coefficient α and incident photon energy ($h\nu$) are given by the equation

$$(\alpha h\nu) = A(h\nu - E_g)^n$$

where, A is a constant, E_g is the bandgap of the material and the exponent n depends on the type of transition. Tauc plots between $(\alpha h\nu)^2$ and energy have been plotted and the linear portions of the graphs were extrapolated to meet the energy axis as shown from Figure 4 from which the energy band gap [11] have been determined as 3.42-3.48 eV. The presence of a single slope in the curves suggests that ZnO nanoparticles are in single phase in nature and the type of transition is direct and allowed. The forbidden band width of the zinc oxide samples produced by zinc nitrate has the minimal value 3.42 eV, which is considerably smaller than that of the product of zinc chloride 3.48 eV. This might be due to the strain arising from chemical synthesis of ZnO nanoparticle. These micro strains highly influence the optical band gap of material.

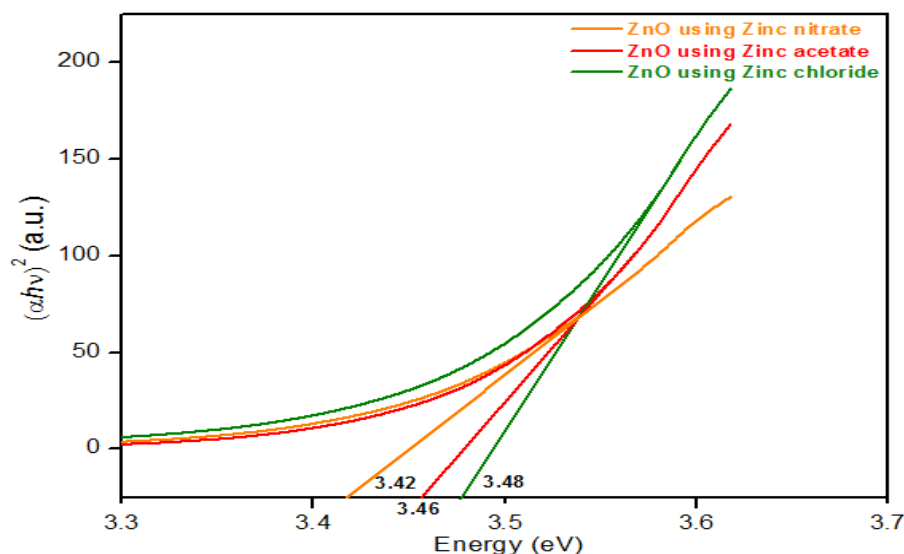


Figure4 Optical bandgap of ZnO nanoparticles

Magnetization- magnetic field (M–H) measurements

The magnetization of the ZnO nanoparticles was performed at room temperature using VSM. The M–H nature of ZnO nanoparticles is shown in Figure 5. At room temperature ZnO samples exhibit diamagnetic characteristics. Magnetic properties of nanoparticles depend on many parameters such as, synthesizing method, grain size, amount and distribution of cations, calcination temperature, oxygen ion occupancy, etc. From the magnetic data it can be inferred that, ferromagnetic property can be achieved in ZnO [12,13] by further introducing Zn_i and/or V_O defects rather than Zn vacancies (V_{Zn}) and confirm which kind of defect plays a more important role in the sample. Because the diffusion of Zn is easier than that of oxygen and there are not enough oxygen atoms from the air which can diffuse in the lattice to oxidize the diffused Zn, Zn_i will generate and be trapped in the lattice, which leads to the increase in defect density of Zn_i . Theoretical calculation indicated that the level of Zn_i lies close to the bottom of the conduction band (shallow donors), which will induce strong interaction between the localized interstitial Zn 4s level and the conduction band. This interaction alternates the electronic structure, leading to ferromagnetic like behavior. It should be noted that this modification of the semiconductor electronic structure can be realized in the absence of the magnetic ions. More generally, other methods inducing such kind of shallow donors will also alternate the electronic structure and result in the ferromagnetism, such as fabricating ZnO low dimensional nanoparticles with more intrinsic defects, capping with organic molecules into ZnO nanoparticle and producing more defects by mechanical milling in ZnO nanoparticles. From the above discussion, diamagnetic behavior of this ZnO samples exhibit less intrinsic defects and it confirms the samples are in phase pure ZnO nanoparticles.

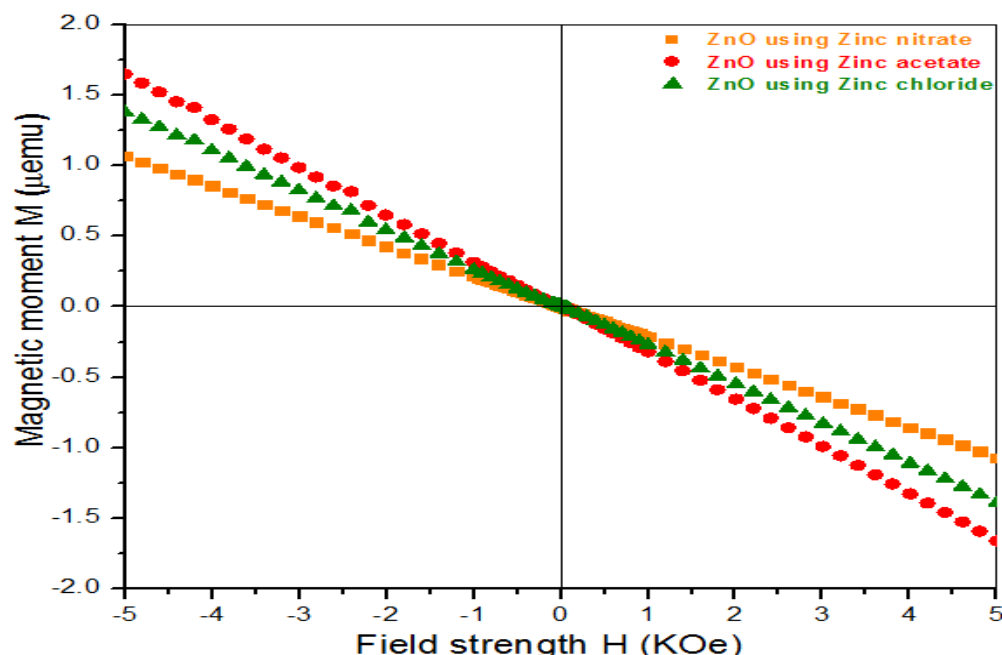


Figure 5. Room temperature (M–H) curves of ZnO samples

Conclusion

Zinc oxide nanoparticles were synthesized by sol-gel method using zinc chloride / zinc acetate dihydrate / zinc nitrate hexahydrate and Sodium Hydroxide as precursors. The XRD patterns ZnO nanoparticles reveal the formation of well-crystalline single phase materials and all ZnO nanoparticles possess hexagonal structure. The lattice parameters were calculated from 2 θ values in the X-ray diffraction patterns by using Fullprof program computer programming. From the results, the unit cell parameters (\AA), unit cell volume (\AA^3) and density (g/cm^3) of ZnO were found to be almost same for various precursor used for synthesis. This confirms, the lattice parameters of the oxides do not depend on the precursor composition. From the investigations of UV-Vis spectra, the excitonic absorption peak at 355-360 nm were observed and have sharp absorption edge which implies the lower particle size of ZnO. The energy band gap have been determined for the samples and found to be 3.42- 3.48 eV. At room temperature ZnO samples exhibit diamagnetic characteristics. The synthesized ZnO samples with various precursors were identified as mesoporous materials and therefore these materials represent a very promising design option for gas sensors and piezoresistive sensors.

References

- 1 Wojnarowicz, J., Chudoba, T. and Lojkowski, W., “A Review of Microwave Synthesis of Zinc Oxide Nanomaterials: Reactants, Process Parameters and Morphologies”, *Nanomaterials*, 10(6), 2020, 1086.
- 2 Vasei, H.V., Masoudpanah, S.M., Adeli, M., Aboutalebi, M.R. and Habibollahzadeh, M., “Mesoporous honeycomb-like ZnO as ultraviolet photocatalyst synthesized via

- solution combustion method”, *Materials Research Bulletin*, 117, 2019, 72-77.
- 3 Fanady, B., Song, W., Peng, R., Wu, T. and Ge, Z., “Efficiency enhancement of organic solar cells enabled by interface engineering of sol-gel zinc oxide with an oxadiazole-based material”, *Organic Electronics*, 76, 2020, p.105483.
- 4 Mishra, P.K., Mishra, H., Ekielski, A., Talegaonkar, S. and Vaidya, B., “Zinc oxide nanoparticles: a promising nanomaterial for biomedical applications”, *Drug discovery today*, 22(12), 2017, 1825-1834.
- 5 Saif, S., Tahir, A., Asim, T., Chen, Y., Khan, M. and Adil, S.F., “Green synthesis of ZnO hierarchical microstructures by *Cordia myxa* and their antibacterial activity”, *Saudi Journal of Biological Sciences*, 26(7), 2019, 1364-1371.
- 6 Chaari, M. and Matoussi, A., “Electrical conduction and dielectric studies of ZnO pellets”, *Physica B: Condensed Matter*, 407(17), 2012, 3441-3447.
- 7 Idris, A.O., Ama, O.M., Ray, S.S. and Osifo, P.O., “Metal Oxide Nanomaterials for Biosensor Application”, In *Nanostructured Metal-Oxide Electrode Materials for Water Purification*, Springer, Cham. 2020, 97-111.
- 8 Ludi, B. and Niederberger, M., “Zinc oxide nanoparticles: chemical mechanisms and classical and non-classical crystallization”, *Dalton Transactions*, 42(35), 2013, 12554-12568.
- 9 Racca, L., Canta, M., Dumontel, B., Ancona, A., Limongi, T., Garino, N., Laurenti, M., Canavese, G. and Cauda, V., “Zinc oxide nanostructures in biomedicine”, In *Smart nanoparticles for biomedicine*, Elsevier, 2018, 171-187.
- 10 Jung, H. and Choi, H., “Catalytic decomposition of ozone and para-Chlorobenzoic acid (pCBA) in the presence of nanosized ZnO”, *Applied Catalysis B: Environmental*, 66(3-4), 2006, 288-294.
- 11 Singh, A.K., Viswanath, V. and Janu, V.C., “Synthesis, effect of capping agents, structural, optical and photoluminescence properties of ZnO nanoparticles”, *Journal of Luminescence*, 129(8), 2009, 874-878.
- 12 Garcia, M.A., Merino, J.M., Fernández Pinel, E., Quesada, A., De la Venta, J., Ruíz González, M.L., Castro, G.R., Crespo, P., Llopis, J., González-Calbet, J.M. and Hernando, A., “Magnetic properties of ZnO nanoparticles”, *Nano letters*, 7(6), 2007, 1489-1494.
- 13 Sun, Y., Zong, Y., Feng, J., Li, X., Yan, F., Lan, Y., Zhang, L., Ren, Z. and Zheng, X., “Oxygen vacancies driven size-dependent d0 room temperature ferromagnetism in well-dispersed dopant-free ZnO nanoparticles and density functional theory calculation”, *Journal of Alloys and Compounds*, 739, 2018, 1080-1088.
14. Amin Salih Mohammed, Saravana Balaji B, Saleem Basha M S, Asha P N, Venkatachalam K(2020),FCO — Fuzzy constraints applied Cluster Optimization technique for Wireless AdHoc Networks,Computer Communications, Volume 154,Pages 501-508.

- 15.Ponmagal, R.S., Karthick, S., Dhiyanesh, B. et al. Optimized virtual network function provisioning technique for mobile edge cloud computing. J Ambient Intell Human Comput (2020).
- 16.Ramamoorthy, S., Ravikumar, G., Saravana Balaji, B. et al. MCAMO: multi constraint aware multi-objective resource scheduling optimization technique for cloud infrastructure services. J Ambient Intell Human Comput (2020).
- 17.Basha, A.J., Balaji, B.S., Poornima, S. et al. Support vector machine and simple recurrent network based automatic sleep stage classification of fuzzy kernel. J Ambient Intell Human Comput (2020)
- 18.Balaji, B.S., Balakrishnan, S., Venkatachalam, K. et al. Automated query classification-based web service similarity technique using machine learning. J Ambient Intell Human Comput (2020)